National Research Institute of Astronomy and Geophysics

NRIAG Journal of Astronomy and Geophysics

www.elsevier.com/locate/nrjag

CrossMark

Implementation of polytropic method to study initial structures of gas giant protoplanets

Gour Chandra Paul [a,*], **Mrinal Chandra Barman** [a], **Abdul Al Mohit** [b]

[a] *Department of Mathematics, University of Rajshahi, Rajshahi 6205, Bangladesh*
[b] *Department of Mathematics, Islamic University, Kushtia 7003, Bangladesh*

Abstract   In this paper we have determined the initial structures of gas giant protoplanets, formed via disk instability, having a mass range of 0.3–10 Jupiter masses by the simple polytropic method. The polytropic protoplanets or polytropes have been assumed to be spheres of solar composition, each of which is in a steady state of quasi-static equilibrium, where the only source of energy is the gravitational contraction of the gas. The results of our calculations for the polytropes with polytropic indices $n = 1$ and $n = 1.5$ are found to be closer to reality and are in good agreement with the findings obtained by other investigations with more rigorous treatment of the problem.
© 2014 Production and hosting by Elsevier B.V. on behalf of National Research Institute of Astronomy and Geophysics.

1. Introduction

With the discovery of extrasolar planets, the interest in planetary system has been rekindled and a large volume of work has been done on the physical conditions prevailing in the interior of such planets both inside and outside the solar system (Guillot, 1999; Hubbard et al., 2002) and researches are still being carried out toward the same. Though, it is now generally agreed that the planets are formed from high orbital angular momentum materials left over from the formation of stars but the details of the formation process are still debated (Hubickyj et al., 2005). Two suggested end viable mechanisms for giant planet formation are core accretion and disk instability. In the core accretion model, a heavy-element core is first formed by accretion of planetesimals, once the core reaches a critical mass ∼10 Earth masses, it can rapidly accrete gas from the surrounding disk to form a gas giant planet (Hubickyj et al., 2005; Pollack et al., 1996; Helled et al., 2006). This mechanism has been adopted as the standard mechanism of planetary formation in both the solar system and in extrasolar planets. Recently, extrasolar planets are discovered by direct imaging (Marois et al., 2008; Kalas et al., 2008). But the standard core accretion model cannot explain properly the formation process of such planets, because it is believed that the gas from the disk disappears before the formation of the massive solid core (Dodson-Robinson et al., 2009). With the difficulties encountered with the core accretion models, the disk instability

* Corresponding author. Tel.: +88 0721 711108; fax: +88 0721 750064.
E-mail addresses: pcgour2001@yahoo.com (G.C. Paul), mcbarman_math@yahoo.com (M.C. Barman), mohit4010@yahoo.com (A.A. Mohit).

Table 1 Central values of thermodynamic variables inside the considered protoplanetary masses for different values of the polytropic index n.

M/M_J	$\rho_c \times 10^{-9}$ (g cm^{-3})				P_c (dyne cm^{-2})				T_c (K)			
	$n = 0$	$n = 0.5$	$n = 1$	$n = 1.5$	$n = 0$	$n = 0.5$	$n = 1$	$n = 1.5$	$n = 0$	$n = 0.5$	$n = 1$	$n = 1.5$
0.3	3.17	5.82	10.43	19.00	17.22	335.58	559.32	772.40	144.84	126.33	144.84	155.99
1.0	3.04	5.59	10.02	18.23	36.31	709.10	1181.87	1632.27	318.83	278.09	318.83	343.37
3.0	2.87	5.26	9.42	17.16	69.83	1360.43	2267.51	4031.02	649.92	556.87	649.92	699.96
5.0	3.82	7.02	12.56	22.91	144.22	2809.59	4682.55	6466.96	1005.83	877.29	1005.81	1083.27
7.0	4.21	7.73	13.85	25.22	205.22	3998.00	6664.11	9202.75	1299.84	1133.73	1299.84	1399.91
10.0	3.41	6.25	11.20	22.40	196.17	3821.57	12738.48	8796.85	1536.17	1339.86	1536.18	1654.44
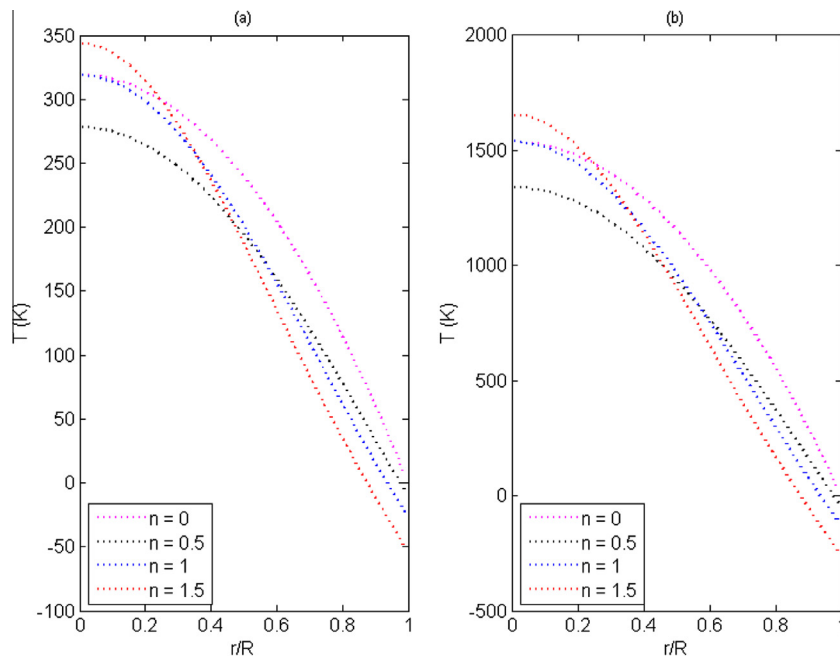
Figure 1 Temperature distributions inside the polytropes with masses 1 M_J and 10 M_J for different values of the polytropic index n; (a) with 1 M_J and (b) with 10 M_J.

model, once in vogue, has been reformulated with fragmentation from massive protoplanetary disks (Nayakshin, 2010; Boley et al., 2010; Cha and Nayakshin, 2011). Although some questions arise as to whether stable protoplanets could form or not, the idea is believed to be a promising route to the rapid formation of giant planets in our solar system and elsewhere (Boss, 2007). Unfortunately, the initial structures of the protoplanets formed via gravitational instability are still unknown and different numerical models can be found to report different configurations (Helled and Schubert, 2008; Helled and Bodenheimer, 2011).

Simulations made by Boss (2002, 2007) predicted colder and less dense objects than the ones found in Mayer et al. (2002, 2004) and the investigations made by both the groups can be found to present warmer and denser initial configurations than the ones used in the investigations of DeCampli and Cameron (1979) and Bodenheimer et al. (1980). However, so far, no author has shown that such protoplanets with definite structures exist in reality. Boss (1998, 2002, 2007), in his

studies, assumed initial protoplanets to be radiative equilibrium, while Helled and Bodenheimer (2011) found the protoplanets to be fully convective with thin radiative outer zones, which is consistent with Bodenheimer et al. (1980). Paul et al. (2012a,b) neglected the thin outer radiative zone and assumed such protoplanets to be fully convective, which can be found to be consistent with (Helled et al., 2005), whereas Paul and Bhattacharjee (2013) and Paul et al. (2013) conducted their investigations assuming the protoplanets to be in conductive-radiative equilibrium. In their investigation Paul et al. (2011) investigated solid grain settling time inside a polytropic protoplanet determining its structure, where they concluded that the segregation time scale obtained by the polytropic method is quite realistic.

In this study we intend to determine the initial structures of gaseous giant protoplanets formed via disk instability having masses between 0.3 and 10 Jovian masses by a simple polytropic method and to see how they compare the findings obtained through different investigations.
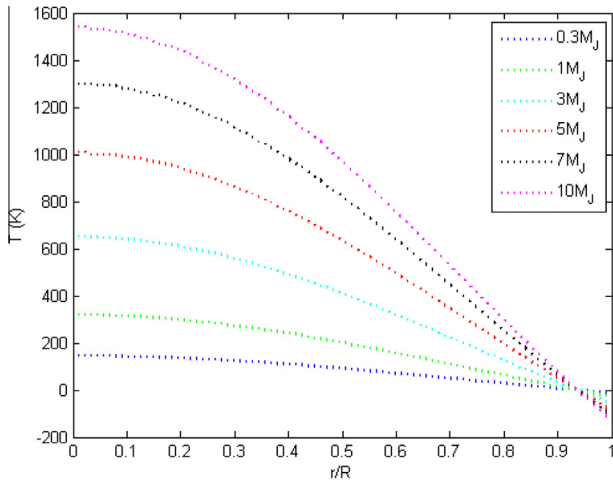
Figure 2 Temperature distributions inside some polytropes with polytropic index $n = 1$.

2. Model equations

Our model assumes a non-rotating, non-magnetic spherical giant gaseous object of solar composition in the mass range of 0.3–10 Jupiter masses. The choice of the mass range is because it covers most of the observed mass range of extrasolar giant planets (Helled and Schubert, 2008). Following Paul et al. (2011), we assume that the object, during its initial stage, contracts quasi-statically (DeCampli and Cameron, 1979; Bodenheimer et al., 1980), which is in a steady state of quasi-static equilibrium, where the gravitational contraction of the gas is only the source of energy. The structure of the object during its initial stage then can be given by the polytropic equation of state (Paul et al., 2011)

$$P = K\rho^{1+1/n}, \tag{1}$$

where n is polytropic index, P is pressure, ρ is density and K is a polytropic constant. It is to be noted here that the solution of this equation gives the stellar structure and correctly represents the behavior of stellar gas. But for polytropic protoplanets, the polytropic index n should sufficiently be small, as initial protoplanets are expected to be less centrally condensed (Paul and Bhattacharjee, 2003).

The distributions of the thermodynamic variables then can be given by the Lane–Emden equation

$$\frac{1}{\xi^2}\frac{d}{d\xi}\left(\xi^2\frac{d\theta}{d\xi}\right) = -\theta^n, \tag{2}$$

subject to the boundary conditions $\theta = 1, \frac{d\theta}{d\xi} = 0$ at $\xi = 0$ (center), where ξ is a dimensionless radius and the dimensionless variable θ is related to the thermodynamic variables ρ, P and T through the relation

$$\theta = \left(\frac{\rho}{\rho_c}\right)^{\frac{1}{n}} = \left(\frac{P}{P_c}\right)^{\frac{1}{1+n}} = \frac{T}{T_c}. \tag{3}$$

Here P_c, ρ_c and T_c are the central pressure, condensation and temperature, respectively, and are given by $\rho_c = a_n\frac{3M}{4\pi R^3}$, $P_c = K\rho_c^{1+1/n}$ and $T_c = c_n\frac{GM}{R}$ for $n = 0.5, 1, 1.5$, whereas for $n = 0$, the central condensation and temperature are obtained using the above respective relation but central pressure can be obtained through the relation $P_c = b_n\frac{GM^2}{R^4}$.

In the above equations, G is the universal gravitational constant, M is the mass of a protoplanet of radius R and a_n, b_n, and c_n are numerical constants having different values for different n. The values of a_n, b_n are available in Menzel et al. (1963) and the values of c_n can be constructed through the formula given below

$$c_n = \frac{4\pi\mu H}{3k}\frac{b_n}{a_n}, \tag{4}$$

where H is the mass of a hydrogen atom, μ is the mean molecular weight and k is the Boltzmann constant.
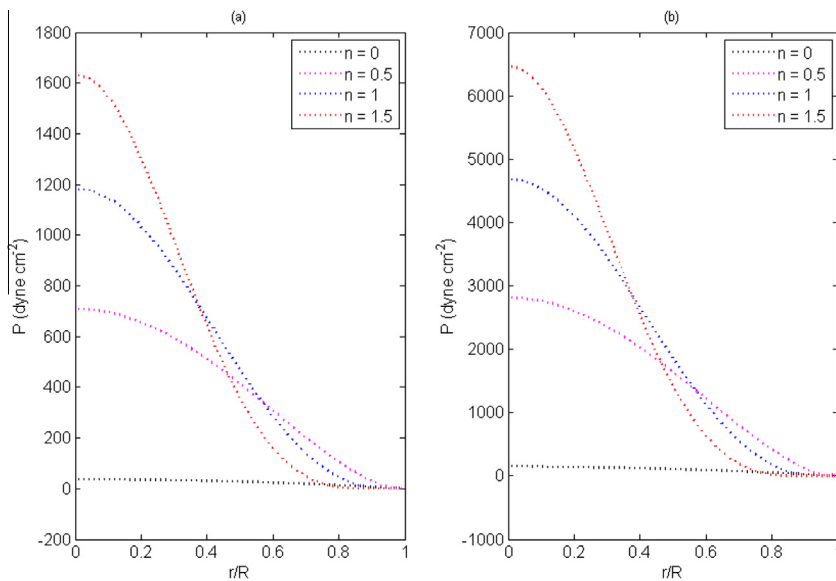

Figure 3 Pressure profiles inside the polytropes with masses 1 M_J and 5 M_J for different values of the polytropic index n; (a) with 1 M_J and (b) with 5 M_J.
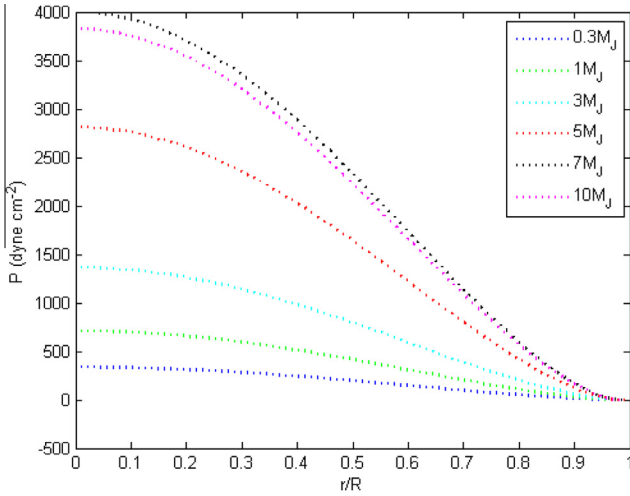
Figure 4 Pressure distributions inside some polytropes with polytropic index $n = 0.5$.

The remaining term, the mass distribution inside a protoplanet can be given by the equation (Paul et al., 2011)

$$\frac{dM(r)}{dr} = 4\pi r^2 \rho, \tag{5}$$

where $M(r)$ is the mass interior to a radius r of a protoplanet.

3. Numerical approach

3.1. Non-dimensionalization

The Eq. (2) was non-dimensionalized with the help of the transformation $\xi = x\xi_1$ and in non-dimensional form, the equation can be put to the form

$$\frac{1}{x^2}\frac{d}{dx}\left(x^2\frac{d\theta}{dx}\right) = -\xi_1^2\theta^n, \tag{6}$$

where ξ_1 is the first zero of the solution to the Lane–Emden.

The necessary boundary conditions then become

$$\theta = 1, \text{and } \frac{d\theta}{dx} = 0 \text{ at } x = 0.$$

Then, the mass distribution given by Eq. (5) with the transformations $r = xR$ and $\xi = x\xi_1$ is reduced to the form

$$M(x) = \frac{4\pi R^3 \rho_c}{\xi_1^2}\left(-x^2\frac{d\theta}{dx}\right). \tag{7}$$

3.2. Solution

The determination of the structure of the protoplanets directly depends on the solution of Eq. (6) and hence Eq. (7). To solve Eq. (6), the parameter n has to be specified. As is mentioned earlier, an initial protoplanet is expected to be less centrally condensed, n is likely to be small. Following Paul et al. (2011) and Paul and Bhattacharjee (2003), we consider four different values of n in our investigation, namely 0, 0.5, 1.0, and 1.5. Inserting the values of necessary parameters involved in Eq. (6) corresponding to the values of n, we have solved it with proper boundary conditions for $n = 0, 0.5, 1.0, 1.5$. As analytic solution of the Lane–Emden equation is not possible for all the assumed values of n, so we have adopted numerical technique. With these values as our initial conditions, we have solved Eq. (6) numerically by the fourth order Runge–Kutta method to determine θ and $\frac{d\theta}{dx}$ for different x. The distributions of the thermodynamic variables ρ, P and T inside the protoplanets with the prescribed masses have been calculated using Eq. (3) and with the corresponding central values presented in Table 1, where the used values of the radii with the corresponding masses in our study are taken from the study of
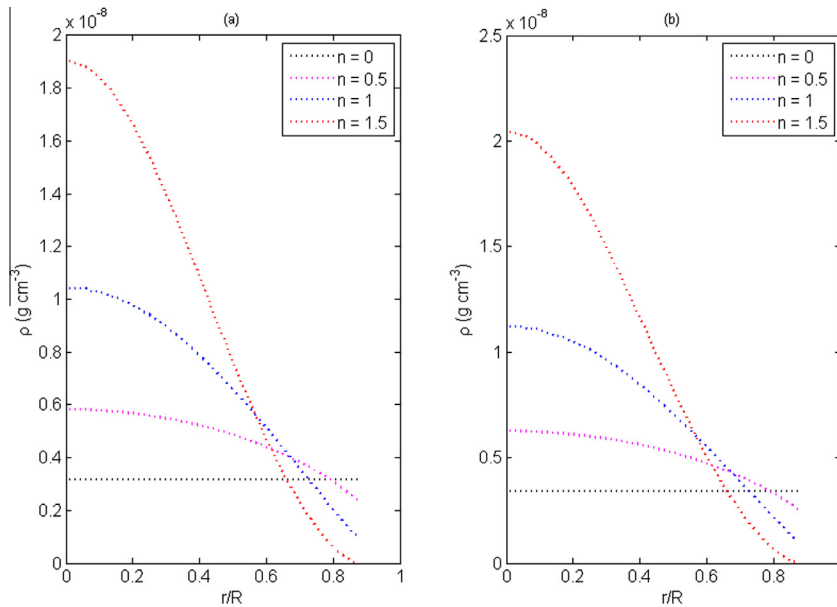

Figure 5 Density distributions inside the polytropes with masses 0.3 M_J and 10 M_J for different values of the polytropic index n; (a) with 0.3 M_J and (b) with 10 M_J.
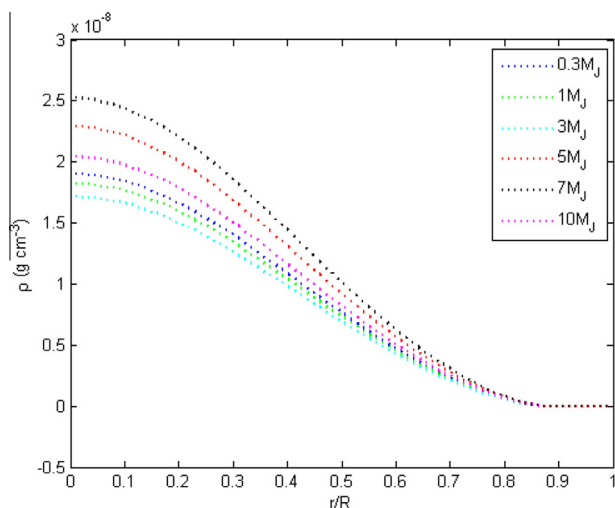
Figure 6   Density distributions inside some polytropes with $n = 1.5$.
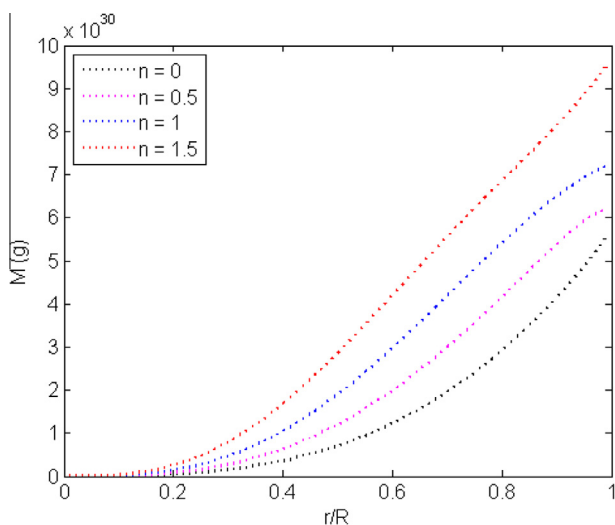

Figure 7   Mass distributions inside a polytrope with mass $3M_J$ for different values of the polytropic index n.

Helled and Schubert (2008). The results of our calculation are shown diagrammatically through Figs. 1–6. The mass distribution is then determined by solving Eq. (7) with the distributions of θ and $\frac{d\theta}{dx}$ for varying x inserting the values of the corresponding parameters involved. Our calculated mass distributions came through our calculation inside some protoplanets for different n are shown in Fig. 7.

4. Results and discussion

Fig. 1 represents temperature profiles of polytropic protoplanets with masses 1 M_J and 10 M_J for different values of the polytropic index n. The diagrams for other polytropes considered generally supported the nature of the diagrams shown in Fig. 1. We think presentations of all such diagrams should

only be space consuming and not physically instructive, and hence they have been excluded. It can be observed from the figure that central temperature inside a protoplanet increases with increasing value of the polytropic index n except when $n = 0$ but surface temperature can be shown to be reduced with the increasing value of the polytropic index n, which can be found to be consistent with the corresponding finding of Paul et al. (2011). Fig. 2 depicts temperature distributions inside all the polytropes with considered masses for the polytropic index $n = 1$. It can be shown from the figure that the more massive is a protoplanet, the hotter is its interior with the same value of the polytropic index n. The temperature profiles inside the polytropes for other polytropic indices generally supported the trend of the corresponding curves shown in Fig. 2. Again due to the similar region mentioned above, they have not been included. However, our presented temperature profiles that come out through calculations for all the considered values of the polytropic index n inside all the polytropes can be found to compare well with the ones presented in Helled and Schubert (2008), Senthilkumar and Paul (2012), Paul and Bhattacharjee (2013) and Paul et al. (2013). Our calculated pressure profiles only for the protoplanetary masses 1 M_J and 5 M_J for different values of the polytropic index n are presented in Fig. 3 and the pressure profiles inside all the polytropic protoplanets with considered masses for the same polytropic index $n = 0.5$ are presented in Fig. 4. Like before, to avoid space consumption, other such corresponding figures related to pressure distribution have been neglected. It can be observed from Fig. 3 that central pressures inside a protoplanet increase with increasing n, whereas for increasing n, the surface pressures can be shown to be reduced. Again, it can be observed from Fig. 4 that the central pressure of a protoplanet depends on its mass and such a pressure increases with increasing mass of the protoplanets except the protoplanet with mass 10 M_J, which can be found to be in excellent accordance with the corresponding finding in Senthilkumar and Paul (2012), Paul and Bhattacharjee (2013), Paul et al. (2013). The pressure distributions obtained in the study with $n = 1$ and 1.5 can be found to compare well with the results presented in Senthilkumar and Paul (2012) and Paul et al. (2013). But the model can be found to predict objects with lower central pressure for $n = 0$ than the ones presented in both the groups.

Fig. 5 depicts our calculated density distributions inside the initial protoplanets with masses 0.3 M_J and 10 M_J having the same considered values of the polytropic index mentioned above, whereas Fig. 6 presents density distributions for the considered masses of the polytropic protoplanets with the same polytropic index $n = 1.5$. Like before, to avoid space consumption, other such corresponding figures related to the density distributions have been excluded. It is seen from Fig. 5 that the central condensation inside a polytrope decreases with increasing polytropic index. It is to be noted here that $n = 0$ represents configuration for the constant density model. Also it is seen from Fig. 5 that while $n = 0.5$, the distributions are flatter almost like a constant density model. It can be observed from Fig. 6 that the protoplanet with mass 10 M_J is rarer than the protoplanet with masses 5 M_J and 7 M_J and the protoplanet with mass 0.3 M_J (Saturn) can be found to be denser than the protoplanets with masses 1 M_J and 3 M_J, which strongly support the findings of Senthilkumar and Paul (2012), Paul and Bhattacharjee (2013) and Paul et al.

(2013). From the figures (Figs. 5 and 6) it is evident that in our model, matter is not uniformly distributed. There is variation of parameters due to variation in density along with gravitational stratification, as is expected for initially formed protoplanets by disk instability. However, the configuration for density distribution obtained in this study for the polytropic protoplanets with considered masses for the two indices $n = 1$ and $n = 1.5$ compares fairly well with the ones obtained in the investigations of Senthilkumar and Paul (2012), Paul and Bhattacharjee (2013) and Paul et al. (2013). But it is pertinent to pin point out here that our obtained density distribution significantly differs with the ones presented in the investigation of Helled and Schubert (2008). In reality, initial configurations of the protoplanets formed via disk instability are still unknown and different numerical models predict different configurations (Helled and Schubert, 2008; Helled and Bodenheimer, 2011).

Fig. 7 represents our calculated mass distributions inside a $3\,M_J$ protoplanet for different values of the polytropic index n. It can be observed from the figure that mass distributions for $n = 1$ and $n = 1.5$ are near to reality. This nature for $n = 1$ and $n = 1.5$ can be shown to be similar for all the protoplanetary masses considered and like before they have not been included to avoid space consumption. In the investigation of Paul and Bhattacharjee (2003), it is seen that if shock wave is the trigger for fragmentation of the nebula, the initial protoplanets are likely be convective. For convection $n = 1.5$. However, it is seen from the diagrams (1, 3, 5, 7) that for $n = 1.5$, the protoplanets have a small envelope and the distributions of variables namely, temperature, pressure, density and mass are quite reasonable which are also true for $n = 1$. However, it is found that for all the considered values of the polytropic index n, the system possesses unique solution suggesting that protoplanets formed via disk instability are a reasonable hypothesis. The findings of our investigation may be important in the study of evolution of extra-solar giant planets.

5. Conclusion and future perspective

Implementation of polytropic method is carried out to investigate the distributions of thermodynamic and physical variables inside protoplanets, formed by gravitational instability, during their initial stage for protoplanetary masses between $0.3\,M_J$ and $10\,M_J$.

Based on the obtained results it can be pointed out here that the investigation of initial structures of the protoplanets formed by disk instability employing polytropic method is quite significant and is reasonable to conclude that the distributions of the thermodynamic and physical variables given by $n = 1$ and $n = 1.5$ are closer to reality. Our future research work will be oriented toward the evolution of extrasolar protoplanets based on the outputs obtained from the study.

Acknowledgments

References

Bodenheimer, P., Grossman, A.S., DeCampli, W.M., Marcy, G., Pollack, J.B., 1980. Calculations of the evolution of the giant planets. Icarus 41, 293–308.

Boley, A.C., Hayfield, T., Mayer, L., Durisen, R.H., 2010. Clumps in the outer disk by disk instability: why they are initially gas giants and the legacy of disruption. Icarus 207, 509–516.

Boss, A.P., 1998. Formation of extrasolar giant planets: core accretion or disk instability? Earth Moon Planets 81, 19–26.

Boss, A.P., 2002. Evolution of the solar nebula. V. Disk instabilities with varied thermodynamics. Astrophys. J. 576, 462–472.

Boss, A.P., 2007. Testing disk instability models for giant planet formation. Astrophys. J. 661, L73–L76.

Cha, S.-H., Nayakshin, S., 2011. A numerical simulation of a "super-Earth" core delivery from ~100 AU to ~8 AU. Mon. Not. R. Astron. Soc. 415, 3319–3334.

DeCampli, W.M., Cameron, A.G.W., 1979. Structure and evolution of isolated giant gaseous protoplanets. Icarus 38, 367–391.

Dodson-Robinson, S.E., Veras, D., Ford, E.B., Beichman, C.A., 2009. The formation mechanism of gas giants on wide orbits. Astrophys. J. 707, 79–88.

Guillot, T., 1999. A comparison of the interiors of Jupiter and Saturn. Planet. Space Sci. 47, 1183–1200.

Helled, R., Kovetz, A., Podolak, M., 2005. Settling of small grains in an extended protoplanet. Bull. Am. Astron. Soc. 37, 675.

Helled, R., Podolak, M., Kovetz, A., 2006. Planetesimal capture in the disk instability model. Icarus 185, 64–71.

Helled, R., Schubert, G., 2008. Core formation in giant gaseous protoplanets. Icarus 198, 156–162.

Helled, R., Bodenheimer, P., 2011. The effects of metallicity and grain growth and settling on the early evolution of gaseous protoplanets. Icarus 211, 939–947.

Hubbard, W.B., Burrows, A., Lunine, J.I., 2002. Theory of giant planets. Annu. Rev. Astron. Astrophys. 40, 103–136.

Hubickyj, O., Bodenheimer, P., Lissauer, J.J., 2005. Accretion of the gaseous envelope of Jupiter around a 5–10 Earth–mass core. Icarus 179, 415–431.

Kalas, P., Graham, J.R., Chiang, E., Fitzgerald, M.P., Clampin, M., Kite, E.S., Stapelfeldt, K., Marois, C., Krist, J., 2008. Optical images of an exosolar planet 25 light-years from Earth. Science 322, 1345–1348.

Marois, C., Macintosh, B., Barman, T., Zuckerman, B., Song, I., Patience, J., Lafrenière, D., Doyon, R., 2008. Direct imaging of multiple planets orbiting the star HR 879. Science 322, 1348–1352.

Mayer, L., Quinn, T., Wadsley, J., Stadel, J., 2002. Formation of giant planets by fragmentation of protoplanetary disks. Science 298, 1756–1759.

Mayer, L., Quinn, T., Wadsley, J., Stadel, J., 2004. The evolution of gravitationally unstable protoplanetary disks: fragmentation and possible giant planet formation. Astrophys. J. 609, 1045–1064.

Menzel, D.M., Bhatnagar, P.L., Sen, H.S., 1963. Stellar interiors. Chapman and Hall Ltd., London.

Nayakshin, S., 2010. A new view on planet formation. arXiv 1012, 1780.

Paul, G.C., Bhattacharjee, S.K., 2003. Structure of protoplanets. J. Ban. Acad. Sci. 27, 161–165.

Paul, G.C., Pramanik, J.N., Bhattacharjee, S.K., 2011. Grain sedimentation time in a gaseous protoplanet. Earth Moon Planets 108, 87–94.

Paul, G.C., Pramanik, J.N., Bhattacharjee, S.K., 2012a. Gravitational settling time of solid grains in gaseous protoplanets. Acta Astronaut. 76, 95–98.

Paul, G.C., Datta, S., Pramanik, J.N., Rahman, M.M., 2012b. Dust grain growth and settling in initial gaseous giant protoplanets. Earth Planets Space 64, 641–648.

Paul, G.C., Bhattacharjee, S.K., 2013. Distribution of thermodynamic variables inside extra-solar protoplanets formed via disk instability. Egypt. J. Remote Sens. Space Sci. 16, 17–21.

Paul, G.C., Rahman, M.M., Kumar, D., Barman, M.C., 2013. The radius spectrum of solid grains settling in gaseous giant protoplanets. Earth. Sci. Inform. 6, 137–144.

Pollack, J.B., Hubickyj, O., Bodenheimer, P., Lissauer, J.J., Podolak, M., Greenweig, Y., 1996. Formation of the giant planets by concurrent accretion of solids and gas. Icarus 124, 62–85.

Senthilkumar, S., Paul, G.C., 2012. Application of new RKAHeM(4,4) technique to analyze the structure of initial extrasolar giant protoplanets. Earth Sci. Inform. 5, 23–31.